Studies on dimension-eight genuine Quartic Boson Coupling operators

A. Marantis[a1], **I. Maznas**[b], **K. Kordas**[b], **A. Leisos**[a], **A. Tsirigotis**[a]

[a] Physics Laboratory, School of Science & Technology, Hellenic Open University, Patras, Greece
[b] Department of Physics, Aristotle University of Thessaloniki, Thessaloniki, Greece

E-mail: alexandros.marantis@cern.ch

July 2021

Abstract. Vector Boson Scattering (VBS) processes provide a great source of information on the structure of the Quartic Gauge Boson Couplings (QGCs). The Standard Model allows self interactions of the charged vector gauge bosons, although vertices with neutral-only bosons are forbidden. In this paper we use Monte Carlo samples containing VBS events with two Z-bosons in association with two jets, and we present preliminary studies for the setting of constraints on anomalous quartic couplings. In these studies we investigate typical kinematic variables and we classify them according to their sensitivity to aQGC effects. Finally, we evaluate the cross-section enhancement by each one of the dimension-eight QGC operators in the ZZjj channel.

1. Introduction

The structure of the Quartic Gauge Couplings (QGCs) is determined by the gauge symmetry $SU(2)_L \otimes U(1)_Y$. The study of the QGCs provides an opportunity to test the Standard Model (SM), while it is also a great source of information for possible indications arising from physics Beyond Standard Model (BSM). QGC processes are studied in the production of electroweak (EWK) vector boson pairs via Vector Boson Scattering (VBS) [1, 2]. The multiboson production and especially the VBS is an effective way to probe the Electroweak Symmetry Breaking (EWSB) sector of the SM [3]. Within the SM, due to cancellations between the Feynman diagrams, the scattering amplitudes involving charged gauge bosons do not grow with the increase of the energy; consequently, there are no unphysical enhancements of cross-sections and violation of the unitarity bounds. In contrast, the couplings between neutral gauge bosons (i.e ZZZZ, ZZZA, ZZAA, ZAAA, AAAA) are forbidden and the deviations from the SM lead to the growth of scattering amplitudes [4]. Therefore, the neutral quartic couplings are characterized as anomalous (aQGCs).

In the case that the $SU(2)_L \otimes U(1)_Y$ symmetry is linearly realized (the case studied in this article), the lowest order QGCs are given by dimension-eight operators, which are called *genuine* QGC operators [5]. For the linear realization of the gauge symmetry, we can construct a low-energy Effective Field Theory (EFT) [6, 7] which can be defined as

[1] Corresponding author

$$\mathcal{L}_{\mathcal{EFT}} = \mathcal{L}_{\mathcal{SM}} + \sum_{d>4} \sum_{i} \frac{f_i}{\Lambda^{d-4}} \mathcal{O}_i \tag{1}$$

where f_i are the Wilson coefficients and d is the dimension of the operators $\mathcal{O}_i$, which involve Higgs doublets, gauge bosons, fermionic fields and covariant derivatives of these fields. In the above parameterization, only the operators with lowest dimensions can contribute significantly below the new physics scale Λ, therefore in the limit $\Lambda \to \infty$ the Lagrangian is composed of SM terms only.

As mentioned above, in this work we are studying the operators that lead to QGCs without Triple Gauge Couplings (TGCs) associated with them. For this reason, we focus to the dimension-eight QGC operators as shown in Table 1. This paper is organized as follows. In Section 2 we present the VBS process and the typical experimental phase space ("fiducial region") which is used to probe the QGCs. In Section 3 we present a study for the sensitivity of the kinematical variables to the QGC effects. Section 4 contains a study which orders the QGC operators for the given VBS process according to their impact on the production cross section. Finally, the results of the studies are discussed in Section 5.

	WWWW	WWZZ	ZZZZ	WWAZ	WWAA	ZZZA	ZZAA	ZAAA	AAAA
$\mathcal{O}_{S,0}$,$\mathcal{O}_{S,1}$	x	x	x						
$\mathcal{O}_{M,0}$, $\mathcal{O}_{M,1}$, $\mathcal{O}_{M,6}$, $\mathcal{O}_{M,7}$	x	x	x	x	x	x	x		
$\mathcal{O}_{M,2}$, $\mathcal{O}_{M,3}$, $\mathcal{O}_{M,4}$, $\mathcal{O}_{M,5}$		x	x	x	x	x	x		
$\mathcal{O}_{T,0}$, $\mathcal{O}_{T,1}$, $\mathcal{O}_{T,2}$	x	x	x	x	x	x	x	x	x
$\mathcal{O}_{T,5}$, $\mathcal{O}_{T,6}$, $\mathcal{O}_{T,7}$		x	x	x	x	x	x	x	x
$\mathcal{O}_{T,8}$, $\mathcal{O}_{T,9}$			x			x	x	x	x

Table 1: Quartic vertices induced by each dim-8 operator.

2. The VBS ZZjj process

The QGC effects in the VBS processes have been studied extensively during the last years at the LHC experiments [8, 9, 10, 11, 12, 13, 14, 15, 16]. In the present analysis we use simulated events and focus on the case of the $ZZjj$ channel at the current LHC centre-of-mass energy of 13 TeV. The $pp \to ZZjj$ events have been produced by the MadGraph5_aMC@NLO [17] generator using the Eboli-Gonzales-Carcia model [18, 5, 1, 19, 2] at leading-order (LO) accuracy; the studies on this paper have been performed at truth level information, without simulating the hadronization process. The studied final state contains four leptons coming from the pair of the Z-bosons and two jets which originate from the deflection of the initial quarks. Representative Feynman diagrams of the EWK $ZZjj$ production are given in Figure 1. In order to imitate the realistic kinematical and geometrical requirements of the ATLAS ZZjj analysis [20], we define a "fiducial" phase-space with kinematic cuts which are optimized to select EWK ZZjj events and limit the QCD contribution. The signal phase-space is defined by the criteria given in the following paragraph.

The transverse momenta p_T for the leading, sub-leading, third and the least energetic lepton are required to be $p_T > 20, 20, 10, 7$ GeV/c, respectively. The absolute pseudorapidity for the electrons must be $|\eta| < 2.47$ and for muons $|\eta| < 2.7$, where the pseudorapidity is defined as $\eta = -\ln\tan(\theta/2)$ where θ is the polar angle with respect to the proton beam axis. In addition, the separation between any two different-flavor leptons is required to be $\Delta R(l, l') > 0.2$, where $\Delta R(l, l') = \sqrt{(\Delta\eta)^2 + (\Delta\phi)^2}$. Possible quadruplets of leptons are constructed by pairing

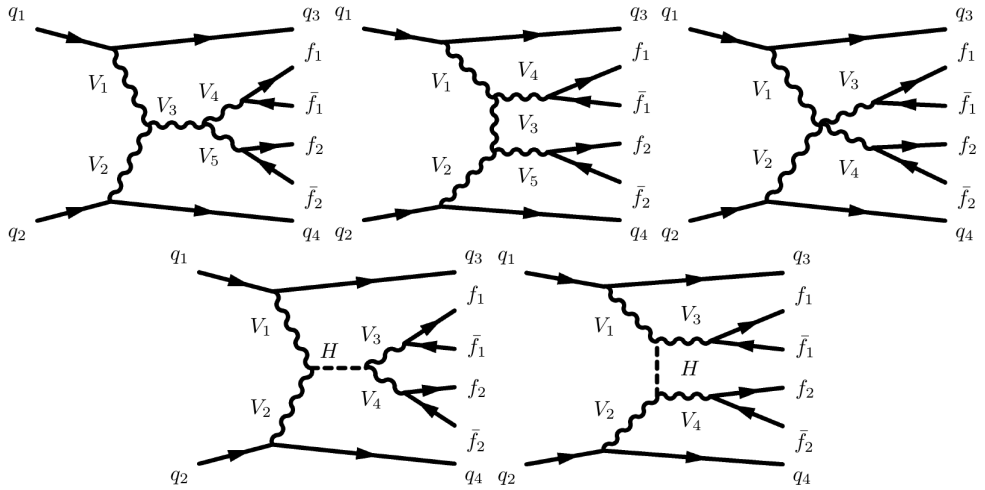

Figure 1: Representative Feynman diagrams of the EWK ZZjj production. The scattering topology includes either a TGC vetex with production of a W/Z boson in the s-channel (top left) and t-channel (top middle), a QGC vertex (top right) or the exchange of a Higgs boson in the s-channel (bottom left) and t-channel (bottom right). The labels V_i refer to the vector bosons (V=W, Z) and f_i to fermions.

same-flavor opposite-sign (SFOS) leptons in order to form Z boson candidates. For the events which contain multiple possible quadruplets, the combination of leptons which minimizes the sum of the absolute differences between the Z boson candidate mass and the Z boson pole mass, $|m_{ll} - m_Z| + |m_{l'l'} - m_Z|$ is selected, with Z boson pole mass being $m_Z = 91.19$ GeV/c^2. Furthermore, the invariant mass of all possible pairs of SFOS leptons must be greater than $m_{ll'} > 10$ GeV/c^2. The Z bosons candidates are required to have mass between 66 GeV/c^2 and 116 GeV/c^2. Finally, for the jets, the transverse momentum is required to be $p_T > 30$ GeV/c and the absolute pseudorapidity $|\eta| < 4.5$. In addition, the jets must be in the backward and forward regions, $\eta_1 \cdot \eta_2 < 0$, meaning that they are well-separated $\Delta\eta_{jj} > 2$. Finally, the invariant mass of the jet system is required to be $m_{jj} > 300$ GeV/c^2.

3. Sensitivity of the kinematical variables to aQGC effects

The extraction of limits on the values of the QGC coefficients uses the distribution of events as a function of a kinematic variable, which typically is the invariant mass of the ZZ system or the p_T of the most energetic ("leading") Z. In this Section, we study the sensitivity of various kinematic variables. For the leading and subleading Z bosons we study their transverse momenta ($p_T^{leadingZ}$, $p_T^{subleadingZ}$) and their centrality ($\zeta_{leadingZ}$, $\zeta_{subleadingZ}$). For the Z-boson pair we study the invariant mass (m_{ZZ}) and the difference in the pseudorapidity ($\Delta\eta_{ZZ}$). Respectively, for the jets we study their invariant mass (m_{jj}) and the difference in the pseusorapidity ($\Delta\eta_{jj}$).

The TMVA toolkit [21] of the ROOT framework is used in order to perform Boosted Decision Trees (BDT) studies to classify the aforementioned kinematic variables. The distributions of the input variables are shown in Figure 2 where the signal (blue) is the QGC contribution and the background (red) is the SM (EWK+QCD) prediction. Both signal and background events have passed the selection criteria mentioned in Section 2.

In the Table 2 the BDT importance of the input variables is presented. The kinematic variables have been sorted according to their sensitivity to the QGC effects. The invariant mass of the Z-boson pair is the most sensitive variable, followed by the p_T of the leading and subleading Z bosons. In all these three cases, the signal enhances the cross-section at the high m_{ZZ} and p_T

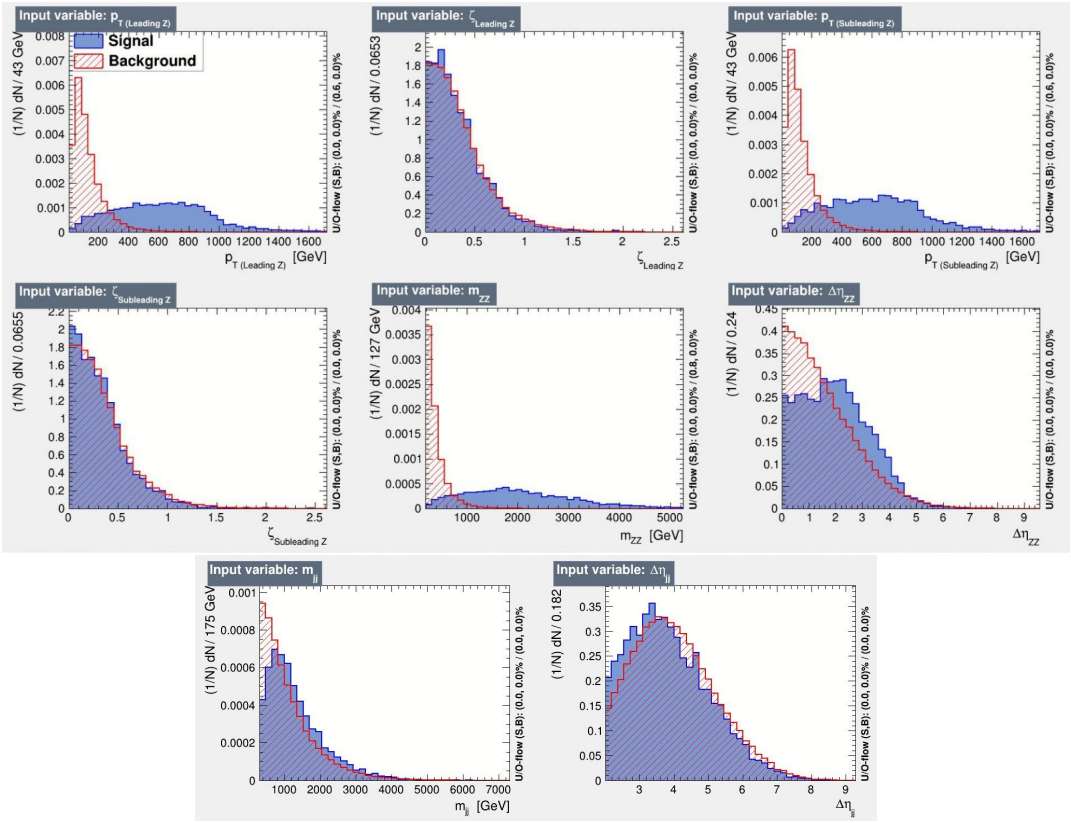

Figure 2: Distributions of the input kinematic variables for the BDT studies, where the signal (blue) is the QGC contribution and the background (red) is the SM prediction.

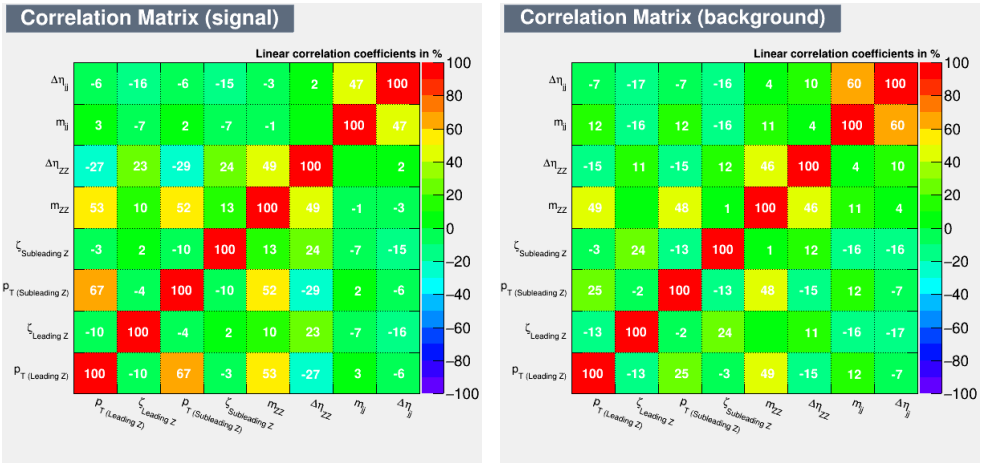

(a) (b)

Figure 3: The colleration between the input kinematic variables for the a) signal and b) background MC events.

values. Finally, the percentage of the linear correlation between the input variables, for both signal and background, is presented in Figure 3.

Rank:	Variable	Variable Importance
	m_{ZZ}	0.1941
	$p_T^{subleadingZ}$	0.1436
	$p_T^{leadingZ}$	0.1388
	$\Delta\eta_{jj}$	0.1094
	$\Delta\eta_{ZZ}$	0.1065
	m_{jj}	0.1034
	$\zeta_{subleadingZ}$	0.1029
	$\zeta_{leadingZ}$	0.1012

Table 2: Ranking of the kinematic variables according to their BDT importance.

4. Sensitivity of dimension-8 operators

Starting from the EFT equation 1, when we include only dimension-8 operators that modify the interactions among electroweak gauge bosons, we get the following Lagrangian

$$\mathcal{L}_{\mathcal{EFT}} = \mathcal{L}_{\mathcal{SM}} + \sum_{j=0,1} \frac{f_{S,j}}{\Lambda^4}\mathcal{O}_{S,j} + \sum_{j=0,\ldots,9} \frac{f_{T,j}}{\Lambda^4}\mathcal{O}_{T,j} + \sum_{j=0,\ldots,7} \frac{f_{M,j}}{\Lambda^4}\mathcal{O}_{M,j} \tag{2}$$

where $\mathcal{O}_{S,j}$, $\mathcal{O}_{M,j}$ and $\mathcal{O}_{M,j}$ are the dimension-8 operators classified in three groups according to the contained number of gauge-boson strength fields. These operators, so-called *genuine* QGC operators, lead to QGCs without a TGC counterpart. The genuine QGC operators can give rise to quartic couplings among neutral gauge bosons. We follow closely ref.[22] and we present in brief the three classes of genuine QGC operators:

Operators containing only $\mathbf{D}_\mu\mathbf{\Phi}$

$$\mathcal{O}_{S,0} = [(D_\mu\Phi)^\dagger D_\nu\Phi] \times [(D^\mu\Phi)^\dagger D^\nu\Phi]$$
$$\mathcal{O}_{S,1} = [(D_\mu\Phi)^\dagger D^\mu\Phi] \times [(D_\nu\Phi)^\dagger D^\nu\Phi]$$

where Φ stands for the Higgs doublet field and $D_\mu \equiv \partial_\mu + i\frac{g'}{2}B_\mu + igW_\mu^i\frac{\tau^i}{2}$ is the covariant derivative where $\tau^i (i = 1, 2, 3)$ represent the $SU(2)_I$ generators with $\mathrm{Tr}\,[\tau^i\tau^j] = 2\delta^{ij}$. These operators contain interactions ($W^+W^-W^+W^-$,W^+W^-ZZ and $ZZZZ$) which do not depend on the gauge boson momenta.

Operators containing only field strength tensors

$$\mathcal{O}_{T,0} = \mathrm{Tr}\,[W_{\mu\nu}W^{\mu\nu}] \times \mathrm{Tr}\,[W_{\alpha\beta}W^{\alpha\beta}]$$
$$\mathcal{O}_{T,1} = \mathrm{Tr}\,[W_{\alpha\nu}W^{\mu\beta}] \times \mathrm{Tr}\,[W_{\mu\beta}W^{\alpha\nu}]$$
$$\mathcal{O}_{T,2} = \mathrm{Tr}\,[W_{\alpha\mu}W^{\mu\beta}] \times \mathrm{Tr}\,[W_{\beta\nu}W^{\nu\alpha}]$$
$$\mathcal{O}_{T,5} = \mathrm{Tr}\,[W_{\mu\nu}W^{\mu\nu}] \times B_{\alpha\beta}B^{\alpha\beta}$$
$$\mathcal{O}_{T,6} = \mathrm{Tr}\,[W_{\alpha\nu}W^{\mu\beta}] \times B_{\mu\beta}B^{\alpha\nu}$$
$$\mathcal{O}_{T,7} = \mathrm{Tr}\,[W_{\alpha\mu}W^{\mu\beta}] \times B_{\beta\nu}B^{\nu\alpha}$$
$$\mathcal{O}_{T,8} = B_{\mu\nu}B^{\mu\nu}B_{\alpha\beta}B^{\alpha\beta}$$
$$\mathcal{O}_{T,9} = B_{\alpha\mu}B^{\mu\beta}B_{\beta\nu}B^{\nu\alpha}$$

where the field strength tensors of the $SU(2)_I$ (W_μ^i) and $U(1)_Y$ (B_μ) respectively, read $W_{\mu\nu} = \frac{i}{2}g\tau^i(\partial_\mu W_\nu^i - \partial_\nu W_\mu^i + g\epsilon_{ijk}W_\mu^j W_\nu^k)$ and $B_{\mu\nu} = \frac{i}{2}g'(\partial_\mu B_\nu - \partial_\nu B_\mu)$. The last two operators $\mathcal{O}_{T,8}$ and $\mathcal{O}_{T,9}$ give rise to quartic couplings containing only neutral gauge bosons (Z,A).

Operators containing both $\mathbf{D}_\mu\mathbf{\Phi}$ and two field strength tensors

$$\begin{aligned}
\mathcal{O}_{M,0} &= \mathrm{Tr}\left[W_{\mu\nu}W^{\mu\nu}\right] \times \left[(D_\beta\Phi)^\dagger D^\beta\Phi\right] \\
\mathcal{O}_{M,1} &= \mathrm{Tr}\left[W_{\mu\nu}W^{\nu\beta}\right] \times \left[(D_\beta\Phi)^\dagger D^\mu\Phi\right] \\
\mathcal{O}_{M,2} &= \left[B_{\mu\nu}B^{\mu\nu}\right] \times \left[(D_\beta\Phi)^\dagger D^\beta\Phi\right] \\
\mathcal{O}_{M,3} &= \left[B_{\mu\nu}B^{\nu\beta}\right] \times \left[(D_\beta\Phi)^\dagger D^\mu\Phi\right] \\
\mathcal{O}_{M,4} &= \left[(D_\mu\Phi)^\dagger W_{\beta\nu}D^\mu\Phi\right] \times B^{\beta\nu} \\
\mathcal{O}_{M,5} &= \left[(D_\mu\Phi)^\dagger W_{\beta\nu}D^\nu\Phi\right] \times B^{\beta\mu} \\
\mathcal{O}_{M,7} &= \left[(D_\mu\Phi)^\dagger W_{\beta\nu}W^{\beta\mu}D^\nu\Phi\right]
\end{aligned}$$

where $W_{\mu\nu}$, $B_{\mu\nu}$, Φ, D_μ are as defined above.

The above 17 genuine QGC operators induce all possible combinations of the vertices VVVV, VVVH and VVHH (where $V = W^\pm, Z^0, A$) which are compatible with the conservation of the C, P and electric charge.

In this study we examine the effect of all $\mathcal{O}_{S,i}$, $\mathcal{O}_{T,i}$, $\mathcal{O}_{M,i}$ operators in order to sort them according to the effect in the total cross section (σ_{tot}). The total amplitude of the process can be expressed as the sum of the SM component and the EFT contributions:

$$|A_{SM} + \sum_i c_i A_i|^2 = |A_{SM}|^2 + \sum_i c_i 2Re(A^*_{SM}A_i) + \sum_i c_i^2|A_i|^2 + \sum_{i,j,i\neq j} c_i c_j 2Re(A_i^* A_j) \qquad (3)$$

where A_{SM} and A_i are the SM and the EFT amplitudes respectively, $c_i 2Re(A^*_{SM}A_i)$ is the interference term between the SM and the EFT operator i, $c_i^2|A_i|^2$ is the pure EFT contribution (quadratic term) and $c_i c_j 2Re(A_i^* A_j)$ is the interference between the EFT coefficients i, j (cross terms).

Assuming only one non-zero coefficient at a time, the interference between the EFT operators (cross term) is zero. Subsequently, we generate independent MC samples of pure EFT and pure SM-EFT interference terms for every coefficient $\lambda = f_i/\Lambda^4$ in the range $[-1, 1]$ TeV^{-4} with a step of 0.1. This way, we create a set of points for each operator and then we perform a quadratic fit to obtain the quadratic function which exhibits the dependence of the cross-section as a function of the value of the coefficient λ. Figures 4,5 and 6 show the sum of the SM-EFT interference and pure EFT total cross section for the operators $\mathcal{O}_{S,i}$, $\mathcal{O}_{T,i}$, $\mathcal{O}_{M,i}$ respectively. The quadratic function of the total cross section (always as function of the QGC coefficient λ) is given in the Tables 3, 4 and 5 where the linear term rises from the SM-EFT interference and the quadratic term from the pure EFT contribution. The ranking of the QGC coefficients according to the contribution in the total cross-section is shown in the Table 6.

Parameter λ (TeV^{-4})	Quadratic function with SM=0 (pb)
f_{S0}/Λ^4	$\sigma(\lambda) = -1.534 \cdot 10^{-5} \cdot \lambda + 2.362 \cdot 10^{-5} \cdot \lambda^2$
f_{S1}/Λ^4	$\sigma(\lambda) = -4.234 \cdot 10^{-6} \cdot \lambda + 3.890 \cdot 10^{-5} \cdot \lambda^2$

Table 3: The total cross section (EFT & SM-EFT Interference) as a function of the f_{Si} coefficients.

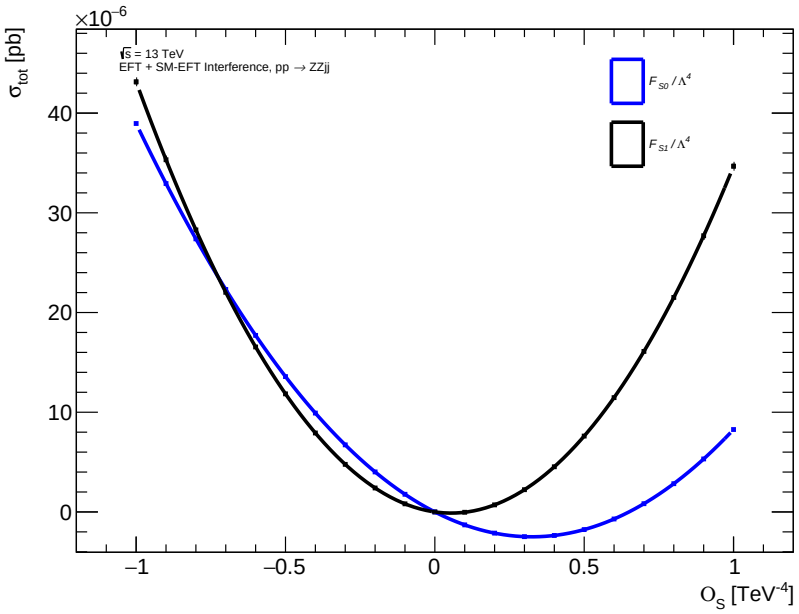

Figure 4: Contribution of EFT and SM-EFT interference terms to the total cross-section (i.e setting the pure SM term to zero) as a function of the f_S/Λ^4 coefficients of the O_S operators.

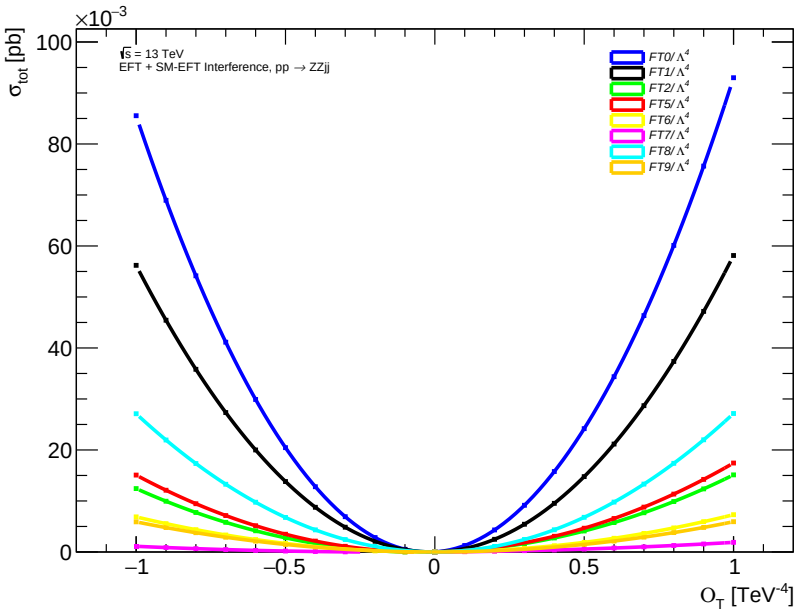

Figure 5: Contribution of EFT and SM-EFT interference terms to the total cross-section (i.e setting the pure SM term to zero) as a function of the f_T/Λ^4 coefficients of the O_T operators.

Parameter λ (TeV^{-4})	Quadratic function with SM=0 (pb)
f_{T0}/Λ^4	$\sigma(\lambda) = 3.725 \cdot 10^{-3} \cdot \lambda + 8.927 \cdot 10^{-2} \cdot \lambda^2$
f_{T1}/Λ^4	$\sigma(\lambda) = 9.646 \cdot 10^{-4} \cdot \lambda + 5.717 \cdot 10^{-2} \cdot \lambda^2$
f_{T2}/Λ^4	$\sigma(\lambda) = 1.342 \cdot 10^{-3} \cdot \lambda + 1.377 \cdot 10^{-2} \cdot \lambda^2$
f_{T5}/Λ^4	$\sigma(\lambda) = 1.180 \cdot 10^{-3} \cdot \lambda + 1.625 \cdot 10^{-2} \cdot \lambda^2$
f_{T6}/Λ^4	$\sigma(\lambda) = 2.145 \cdot 10^{-4} \cdot \lambda + 7.094 \cdot 10^{-3} \cdot \lambda^2$
f_{T7}/Λ^4	$\sigma(\lambda) = 3.868 \cdot 10^{-4} \cdot \lambda + 1.495 \cdot 10^{-3} \cdot \lambda^2$
f_{T8}/Λ^4	$\sigma(\lambda) = 2.265 \cdot 10^{-5} \cdot \lambda + 2.713 \cdot 10^{-2} \cdot \lambda^2$
f_{T9}/Λ^4	$\sigma(\lambda) = 1.323 \cdot 10^{-5} \cdot \lambda + 5.918 \cdot 10^{-3} \cdot \lambda^2$

Table 4: The total cross section (EFT & SM-EFT Interference) as a function of the f_{Ti} coefficients.

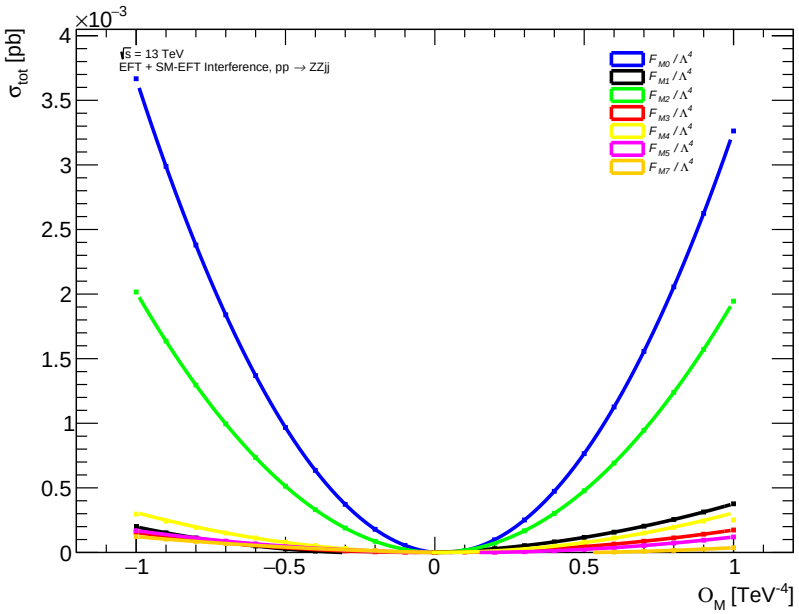

Figure 6: Contribution of EFT and SM-EFT interference terms to the total cross-section (i.e setting the pure SM term to zero) as a function of the f_M/Λ^4 coefficients of the O_M operators.

Parameter λ (TeV^{-4})	Quadratic function with SM=0 (pb)
f_{M0}/Λ^4	$\sigma(\lambda) = -2.022 \cdot 10^{-4} \cdot \lambda + 3.464 \cdot 10^{-3} \cdot \lambda^2$
f_{M1}/Λ^4	$\sigma(\lambda) = 8.939 \cdot 10^{-5} \cdot \lambda + 2.872 \cdot 10^{-4} \cdot \lambda^2$
f_{M2}/Λ^4	$\sigma(\lambda) = -3.569 \cdot 10^{-5} \cdot \lambda + 1.980 \cdot 10^{-3} \cdot \lambda^2$
f_{M3}/Λ^4	$\sigma(\lambda) = 9.496 \cdot 10^{-6} \cdot \lambda + 1.641 \cdot 10^{-4} \cdot \lambda^2$
f_{M4}/Λ^4	$\sigma(\lambda) = -2.280 \cdot 10^{-5} \cdot \lambda + 2.741 \cdot 10^{-4} \cdot \lambda^2$
f_{M5}/Λ^4	$\sigma(\lambda) = -2.452 \cdot 10^{-5} \cdot \lambda + 1.443 \cdot 10^{-4} \cdot \lambda^2$
f_{M7}/Λ^4	$\sigma(\lambda) = -4.305 \cdot 10^{-5} \cdot \lambda + 7.934 \cdot 10^{-5} \cdot \lambda^2$

Table 5: The total cross section as a function of the f_{Mi} coefficients.

Rank	QGC coefficient λ (TeV^{-4})	σ_{tot} (fb) for $\lambda = 1$ TeV^{-4}
1.	f_{T0}/Λ^4	92.995
2.	f_{T1}/Λ^4	58.135
3.	f_{T8}/Λ^4	27.153
4.	f_{T5}/Λ^4	17.430
5.	f_{T2}/Λ^4	15.112
6.	f_{T6}/Λ^4	7.309
7.	f_{T9}/Λ^4	5.931
8.	f_{M0}/Λ^4	3.262
9.	f_{M2}/Λ^4	1.944
10.	f_{T7}/Λ^4	1.882
11.	f_{M1}/Λ^4	0.377
12.	f_{M4}/Λ^4	0.251
13.	f_{M3}/Λ^4	0.174
14.	f_{M5}/Λ^4	0.130
15.	f_{M7}/Λ^4	0.036
16.	f_{S1}/Λ^4	0.035
17.	f_{S0}/Λ^4	0.0008

Table 6: Ranking of the QGC coefficients according to their contribution it the total cross-section of the EWK ZZjj process, where the pure SM contribution is set to zero.

5. Conclusions

Vector Boson Scattering processes are sensitive to deviations from the SM predictions originating from anomalous Quartic Gauge Couplings. A useful methodology followed by the LHC experiments is the parametrization of such deviations in the context of an Effective Field Theory which in the QGC case involves dimension-eight operators. In this paper we examined first the utilization of various kinematic variables as probes for the existence of anomalous QGCs; the most sensitive variable is found to be the invariant mass of the Z-boson pair. Then, we investigated the contribution in the total cross-section of the EWK ZZjj process from each one of the QGC operators and we classified them according to their sensitivity. The findings of both studies are summarized in Tables 2 and 6.

Acknowledgments

The research work was supported by the Hellenic Foundation for Research and Innovation (HFRI) and the General Secretariat for Research and Technology (GSRT), under the HFRI PhD Fellowship Grant GA. no. 677.

References

[1] Eboli O J P, Gonzalez-Garcia M C, Lietti S M and Novaes S F 2001 *Phys. Rev. D* **63** 075008
[2] Eboli O J P, Gonzalez-Garcia M C and Lietti S M 2004 *Phys. Rev. D* **69** 095005
[3] Brivio I, Corbett T, Éboli O J P, Gavela M B, Gonzalez-Fraile J, Gonzalez-Garcia M C, Merlo L and Rigolin S 2014 *JHEP* **03** 024
[4] Cornwall J M, Levin D N and Tiktopoulos G 1975 *Phys. Rev. D* **11**(4) 972–972
[5] Éboli O J P, Gonzalez-Garcia M C and Mizukoshi J K 2006 *Phys. Rev. D* **74**(7) 073005
[6] Georgi H 1993 *Ann. Rev. Nucl. Part. Sci.* **43** 209–252
[7] 2013 *Annals of Physics* **335** 21–32 ISSN 0003-4916
[8] Aad G *et al.* (ATLAS) 2014 *Phys. Rev. Lett.* **113** 141803
[9] Khachatryan V *et al.* (CMS) 2015 *Phys. Rev. Lett.* **114** 051801
[10] Khachatryan V *et al.* (CMS) 2017 *Phys. Lett. B* **770** 380–402
[11] Aaboud M *et al.* (ATLAS) 2017 *JHEP* **07** 107
[12] Sirunyan A M *et al.* (CMS) 2017 *Phys. Lett. B* **774** 682–705
[13] Sirunyan A M *et al.* (CMS) 2021 *Phys. Lett. B* **812** 135992
[14] Aaboud M *et al.* (ATLAS) 2017 *Phys. Rev. D* **95** 032001
[15] Sirunyan A M *et al.* (CMS) 2019 *Phys. Lett. B* **795** 281–307
[16] Sirunyan A M *et al.* (CMS) 2018 *Phys. Rev. Lett.* **120** 081801
[17] Alwall J, Herquet M, Maltoni F, Mattelaer O and Stelzer T 2011 *JHEP* **06** 128
[18] Belyaev A S, Eboli O J P, Gonzalez-Garcia M C, Mizukoshi J K, Novaes S F and Zacharov I 1999 *Phys. Rev. D* **59** 015022
[19] Éboli O J P and Gonzalez-Garcia M C 2016 *Phys. Rev. D* **93** 093013
[20] Aad G *et al.* (ATLAS) 2020 Observation of electroweak production of two jets and a Z-boson pair with the ATLAS detector at the LHC
[21] Hocker A *et al.* 2007 TMVA - Toolkit for Multivariate Data Analysis Tech. rep.
[22] Baak M *et al.* 2013 Working Group Report: Precision Study of Electroweak Interactions *Community Summer Study 2013: Snowmass on the Mississippi*